

# Nonequilibrium phononic first-order phase transition in a driven fermion chain

Mohsen Yarmohammadi,<sup>1,\*</sup> Marin Bukov,<sup>2,†</sup> and Michael H. Kolodrubetz<sup>1,‡</sup>

<sup>1</sup>*Department of Physics, The University of Texas at Dallas, Richardson, Texas 75080, USA*

<sup>2</sup>*Max Planck Institute for the Physics of Complex Systems, Nöthnitzer Str. 38, 01187 Dresden, Germany*

(Dated: October 11, 2024)

We study the direct laser drive of infrared-active phonons that are quadratically coupled to a spinless fermion chain. Feedback is incorporated by phonon dressing of the electronic dispersion, which enables effective non-linearities in the phonon dynamics. We uncover a first-order phase transition in the phononic steady state in which hysteretic effects allow either large or small phonon occupation depending on the drive protocol. We discuss the implications of these findings for probing phase transitions in real driven materials.

*Introduction.*—Despite a considerable ongoing effort to understand quantum systems, uncovering nonequilibrium phenomena without an apparent equilibrium analogue is one of the outstanding scientific challenges in modern condensed matter physics. Recent developments in the ultrafast dynamics of quantum materials have attracted interest in exploring novel nonequilibrium many-body phenomena [1–7]. Interacting light-matter systems with competing interactions emerged as a useful experimental platform since they allow to study the interplay between coupling to an environment and external drives [8–10]. Moreover, they play a central role in the study of photovoltaics [11, 12], light-induced phase transitions [13, 14], and laser processing [15].

Direct laser driving of an infrared (IR)-active phonon is the main light-matter interaction channel; it couples to the electron degree of freedom by modifying its environment. In a typical setup, phonons couple to the electron number operator in a nonlinear manner [16]. Over the last decade, a considerable effort has been devoted to studying the role of electron-phonon coupling on the dynamical properties of high-temperature cuprate superconductors [17, 18] and Mott or charge-density-wave insulators [19–22]. For a driven electron-phonon system to avoid heating (e.g., with the goal to store and transmit information), the latter needs to be counterbalanced by dissipation from undriven phonon modes. This has been studied in spin lattices [23–25], coupled quantum-electrodynamics cavities and circuits [26–28], lattice Rydberg atoms [29–31], driven-dissipative superfluids [32], nonlinear photonic modes [33, 34], etc. Although dissipation is widely captured in the dynamics of local observables, a detailed understanding of the process is still an outstanding challenge.

Studies of interacting systems, exposed to an external laser field and coupled to a thermal bath, have until recently mostly focused on the “bare” dispersion of degrees of freedom in dissipation processes. However, it remains to be understood how the backaction of transient excitations can be incorporated into the dissipation process. To the best of our knowledge, this has not been addressed so far in phononically driven materials. This mainly requires a deep scan of the “dressed” electronic dispersion

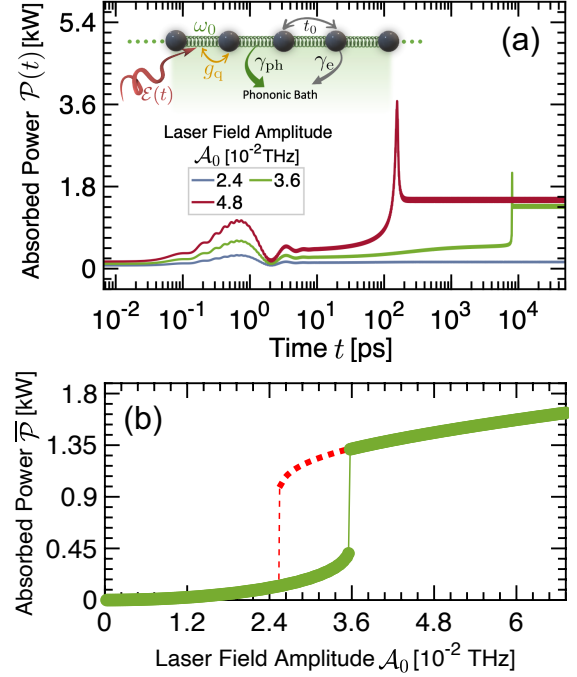


**FIG. 1. Nonequilibrium first-order phase transition in a phononically driven fermion chain.** (a) Drive-period-averaged time evolution of absorbed power for a driven-dissipative chain of spinless fermions, sketched in the inset, starting from the ground state at half filling. The system reaches a nonequilibrium steady state (NESS) which undergoes a first-order phase transition at laser amplitude  $\mathcal{A}_0 \approx 3.6 \times 10^{-2}$  THz [solid line in (b)] due to phononic modification of the electronic dispersion. The dashed line in (b) shows a second stable NESS which can be created by modifying either the initial state or drive protocol. The parameters are chosen to be  $\omega = 4.44$  THz,  $\omega_0 = 4.8$  THz,  $g_q = 9.6$  THz,  $\gamma_{\text{ph}} = 0.24$  THz, and  $\gamma_e = 0.0024$  THz; see text for details.

through a time-dependent damping rate, which results in a novel physical insight.

In this Letter, we show that a driven-dissipative fermion chain with a dressed dispersion, exhibits a *dynamical first-order phase transition* due to local depopulation of the electrons in the spirit of quadratic electron-phonon coupling (QEPC). One experimental signature of

the transition is a sharp spike in the long time-evolution of the absorbed power, accompanied by a discontinuity in its value in the long-time nonequilibrium steady state (NESS), as shown in Fig. 1. We analyze and identify accessible parameter regimes to provide a clear path for experimental verification.

*Model.*—Consider an infinite half-filled chain of spinless fermions with periodic boundary conditions, as illustrated in Fig. 1(a), inset. We drive the chain by a continuous field coupled to the IR-active optical phonons, which illuminates the entire system until it reaches a NESS. The model Hamiltonian reads [35–37]

$$\mathcal{H}(t) = -t_0 \sum_{\ell} (c_{\ell}^{\dagger} c_{\ell+1} + \text{H.c.}) + \omega_0 \sum_{\ell} a_{\ell}^{\dagger} a_{\ell} + g_q \sum_{\ell} (a_{\ell}^{\dagger} + a_{\ell})^2 (c_{\ell}^{\dagger} c_{\ell} - 1/2) + \mathcal{E}(t) \sum_{\ell} (a_{\ell}^{\dagger} + a_{\ell}), \quad (1)$$

where  $c_{\ell}^{\dagger}$  ( $c_{\ell}$ ) and  $a_{\ell}^{\dagger}$  ( $a_{\ell}$ ) are respectively the electron and phonon creation (annihilation) operators at lattice site  $\ell$ ;  $t_0$  is a constant hopping amplitude setting the energy scale of our model,  $\omega_0$  is the optical phonon frequency,  $c_{\ell}^{\dagger} c_{\ell} - 1/2$  is the electron number operator relative to half filling, and  $g_q$  is the strength of QEPC. In the laser-phonon coupling, the laser field is described by  $\mathcal{E}(t) = \mathcal{A}_0 \cos(\omega t)$  with frequency  $\omega$  and amplitude  $\mathcal{A}_0$ . In momentum space, we have the bare electronic dispersion  $\omega_k = -2t_0 \cos k$  and a  $k$ -independent phonon frequency; the full  $k$ -space Hamiltonian is provided in Sec. S1 of the Supplemental Material (SM) [38].

We focus our simulations on the dynamics of the approximate dispersionless phonon (assuming a flat band for Einstein phonons), since in most materials, the average  $\omega_0$  is much larger than the phonon bandwidth. Due to the relatively long wavelength of the drive phonons compared to the lattice spacing, the phonon response is dominated by the zero momentum mode  $a_0$ , see Sec. S2 of the SM. We also neglect linear and higher electron-phonon coupling effects, since in target centrosymmetric structures [36, 37] the dominant coupling is quadratic, see Sec. S3 of the SM for the negligible contribution of LEPC due to a vanishing average of linear oscillations. For comparison to experiments on materials with nonlinear electron-phonon coupling, we choose to consider a representative hopping energy  $t_0 = 10 \text{ meV} \approx 2.4 \text{ THz}$ , which can also be chosen to be similar to (Pb,Bi)<sub>2</sub>Sr<sub>2</sub>CaCu<sub>2</sub>O<sub>8</sub>, YBa<sub>2</sub>Cu<sub>3</sub>O<sub>6+x</sub>, and K<sub>3</sub>C<sub>60</sub> [36, 39–41] without qualitatively modifying the results.

The system is coupled to a phononic bath (given by independent phonon modes not subject to the drive) which allows the formation of a NESS. To model the dynamics of the dissipation process, we use the Lindblad master equation with conventional local jump operators,  $(a_0^{\dagger}, a_0)$  and  $(c_k^{\dagger}, c_k)$ , and decoherence rates,  $\gamma_{\text{ph}}$  and  $\gamma_e$ , which relax the phonons and electrons, respectively, to thermal equilibrium [25, 42–44]. We consider relaxation toward zero temperature which, crucially, depends on the state

of the phonons and electrons via the QEPC. Therefore, as the phonon fluctuations  $(a_0^{\dagger} + a_0)^2$  become large, they shift the chemical potential of the electrons downward, modifying the NESS electron density in the region where the laser drive couples. Moreover, we assume that the chain is in touch with a cooling apparatus [25] to remediate the heating created by the continuous drive. Although our results are robust to the parameters chosen, we consider the experimentally relevant  $\omega_0 = 4.8 \text{ THz}$ ,  $\gamma_{\text{ph}} = 0.24 \text{ THz}$ , and  $\gamma_e = 0.0024 \text{ THz}$  throughout the text, unless otherwise specified.

We initialize the system in its ground state (electrons at half filling, phonons in the vacuum state), and let it evolve in time following the Lindblad formalism [42, 43]. We perform numerical simulations for chain lengths up to  $L = 1001$  sites. A complete derivation of the equations of motion governing the time evolution of the system’s observables can be found in Sec. S2 of the SM.

As the QEPC  $g_q$  plays an essential role in determining the dynamics of the model, it is worth noting that the renormalization of the phonon frequency in our model, i.e.,  $\tilde{\omega}_0 = \omega_0 \sqrt{1 + 4g_q[\langle n_{e,\ell} \rangle - 1/2]}/\omega_0$  does not lead to instabilities in the simulation, in contrast to other works [36, 37] where the system is unstable for  $|g_q| > \omega_0/2$ . The reason for this is our mean-field-type approximation, which replaces the quantized on-site electron occupation by an average value that only weakly deviates from 1/2. Crucially, this lack of instability is also physical, suggesting that our results will survive fluctuations. This is because the constraint  $|g_q| > \omega_0/2$  comes from the assumption of dispersionless Einstein phonons; in reality, there will always be some finite dispersion, causing excitations of the phonons to be spread over at least a few sites. If the minimal spatial dispersion is  $\ell$  sites, the instability threshold should be roughly increased by a factor of  $\ell$ , which brings it well above the value for  $g_q$  in real materials. Hence, our approximation allows us to simulate the model for arbitrary QEPC strength.

*Results.*—Upon quenching on the drive and solving the dynamics, the system evolves into a NESS as seen in Fig. 1(a) and Sec. S3 of the SM. For the majority of parameters, it takes around 600 ps to reach the NESS, which is within the current technological capabilities of laser sources in ultrafast experiments. To remove fast oscillations, we often average an observable  $O(t)$  over one drive period, denoted by  $\bar{O}$ . In addition to microscopic parameters such as electron and phonon occupation, we consider the NESS energy flow from the drive into the final stage of dissipation for various degrees of freedom (see Sec. S4 of the SM). Of particular importance is the absorbed power

$$\mathcal{P}(t) = -w a \rho \omega_0 \mathcal{E}(t) p_{\text{ph}}(t), \quad (2)$$

where  $p_{\text{ph}}(t) = L^{-1/2} \langle i(a_0^{\dagger} - a_0) \rangle(t)$  denotes the phonon momentum. We use parameters from the YBCO sam-

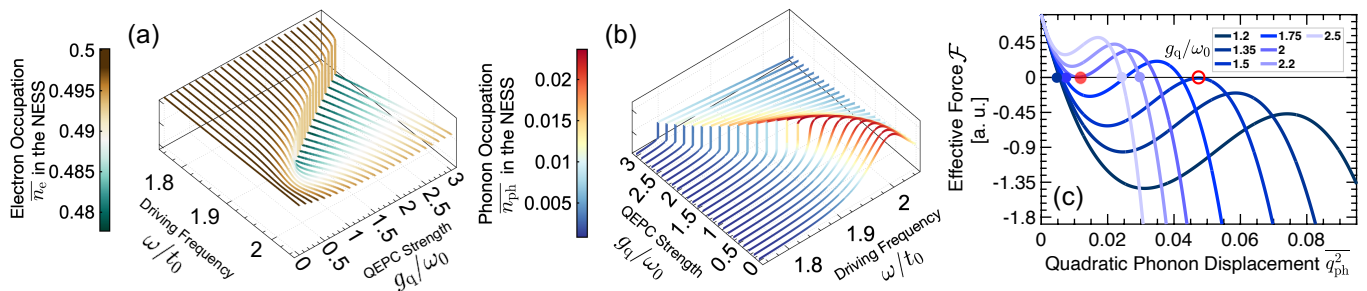


FIG. 2. **Origin of nonequilibrium first-order phase transition.** Dynamical response of dressed (a) electron and (b) phonon occupations in the nonequilibrium steady state for various quadratic electron-phonon couplings and driving frequencies (axes are swapped in (b) to improve visibility of jumps at the phase transition). Depopulation of the electrons leads to shifting of the phonon resonance, a nonlinearity which enables a first-order phase transition in the NESS at strong  $g_q$ . (c) Nonequilibrium effective force (see text) for various  $g_q$  at driving frequency  $\omega = 4.44$  THz, which is below the bare phonon frequency. Shaded blue dots indicate the numerical steady state. Red dots indicate the two predicted phase transitions (see text), with bistability for  $3/2 < g_q/\omega_0 < 2$ . Parameters are  $\omega_0 = 4.8$  THz,  $\mathcal{A}_0 = 0.036$  THz,  $\gamma_{\text{ph}} = 0.24$  THz, and  $\gamma_e = 0.0024$  THz.

ple [45], namely thickness  $w = 10$  nm, area  $a = 1$  mm<sup>2</sup>, and molar density  $\rho \approx 0.007$  mol.cm<sup>-3</sup>. This power is related to experimentally measurable quantities such as reflectance [46–53].

We begin by discussing the response of the electrons and phonons to changing drive frequency  $\omega$  and QEPC  $g_q$  [Figs. 2(a) and 2(b)]. In the absence of QEPC, there is a resonant peak at  $\omega = \omega_0$ , more clearly visible in the phonon occupation. As  $g_q$  is increased, the peak shifts to the lower frequency, which comes from the depopulation of the electronic modes via feedback from the phonons. Surprisingly, above a critical value of  $g_q$ , the smooth peak suddenly becomes a sharp jump, suggestive of a first-order phase transition. At this transition point, the time-evolved observables undergo a non-analytic change, exhibiting a sharp peak at long times as seen in Fig. 1(a).

As we show later, modifying either the initial state or the drive protocol leads to a different NESS, as shown by the dashed red line in Fig. 1(b) and supported by the data in Fig. 4.

The main origin of the phase transition is dissipation-induced nonlinearity. The dressed electron dispersion  $\tilde{\omega}_k(t) = \omega_k + g_q \overline{q_{\text{ph}}^2}(t)$  will yield an average shift of the electron chemical potential given by  $g_q \overline{q_{\text{ph}}^2}$  (note that  $\overline{q_{\text{ph}}} = 0$ ), where  $q_{\text{ph}}(t) = L^{-1/2}(a_0^\dagger + a_0)(t)$  is the phonon displacement. Defining the electron density  $n_e(t) = L^{-1} \sum_k \langle c_k^\dagger c_k \rangle(t)$  and linearizing around the Fermi surface, we predict a steady state electron density of

$$\overline{n}_e = \frac{1}{2} - \frac{g_q \overline{q_{\text{ph}}^2}}{2\pi t_0}. \quad (3)$$

Similarly, the electron occupation shifts the effective phonon frequency to  $\tilde{\omega}_0(t) = \omega_0 \sqrt{1 + 4g_q [n_{e,k}(t) - 1/2] / \omega_0}$  [54]. Since the steady state to which the electrons attempt to relax to depends on the phonon state, whose dynamics, in turn, depend on the electron density, this results in effective

nonlinearities in the dynamics. This backaction was not considered in previous works [36, 37] because the electron was assumed to relax to its undriven ground state. While reasonable for linear electron-phonon coupling, the presence of a finite  $\overline{q_{\text{ph}}^2}$  makes this backaction crucial for QEPC through the Fermi-Dirac mean number [55]. Correctly accounting for this backaction is our major contribution to the model which, as we have seen, produces significant effects on the dynamics. It is also important to note that  $\overline{q_{\text{ph}}^2}(t)$  can be experimentally measured through the intensity of a diffraction peak in femtosecond time-resolved X-rays [56], enabling another path to measure the effects of this backaction.

To microscopically interpret the observed phase transition, we consider the system near its steady state; we assume that the phonons synchronize with the drive, with complex Fourier component of displacement  $q_1 e^{i\omega t}$ , where  $\overline{q_{\text{ph}}^2} = |q_1|^2/2$ . Away from the NESS,  $q_1$  slowly evolves towards a stationary point, which can be obtained by setting  $\dot{q}_{\text{ph}} = 0$ . As shown in Sec. S5 of the SM, this gives a cubic equation that may be thought of as an effective force acting on the phonon near the NESS:

$$\mathcal{F}(\mathcal{X}) = -\frac{4g_q^4 \omega_0^2}{\pi^2 t_0^2} \mathcal{X}^3 - \frac{4g_q^2 \omega_0}{\pi t_0} \left( \omega^2 - \omega_0^2 + \frac{\gamma_{\text{ph}}^2}{4} \right) \mathcal{X}^2 - \left( \gamma_{\text{ph}}^2 \omega^2 + (\omega^2 - \omega_0^2)^2 \right) \mathcal{X} + 2\mathcal{A}_0^2 \omega_0^2, \quad (4)$$

where  $\mathcal{X} = \overline{q_{\text{ph}}^2}$ . Steady states out of equilibrium correspond to solutions of  $\mathcal{F}(\mathcal{X}) = 0$ ; stable attractors have  $d\mathcal{F}/d\mathcal{X} < 0$ . As seen in Fig. 2(c), the force curve shifts depending on various parameters and appears to have two separate phase transitions (marked by red circles) from having a unique NESS to a regime with two distinct stable NESSs. The first phase transition (transparent circle) is visible in our numerical data since, starting from a vacuum state, a jump from small to large  $\overline{q_{\text{ph}}^2}$  matches our expectations. The second phase transition (open circle) is not seen in the data, but could be realized via proto-

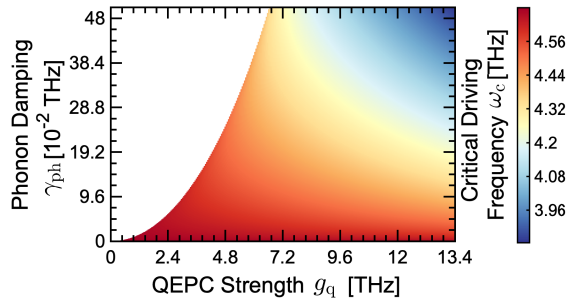


FIG. 3. **Dynamical damping-coupling constraint for the phase transition.** Critical driving frequency as a function of phonon damping rate and strength of quadratic electron-phonon coupling at  $\omega_0 = 4.8$  THz,  $\mathcal{A}_0 = 0.036$  THz, and  $\gamma_e = 0.0024$  THz. The transition occurs down to arbitrarily small values of  $g_q$  and  $\gamma_{\text{ph}}$ . The separatrix, below which dynamical first-order phase transitions occur, is parabolic in the  $\gamma_{\text{ph}} - g_q$  plane.

cols similar to those in Fig. 4. This bifurcation transition with a cubic equation for the effective force is reminiscent of the magnetization in a first-order Ising phase transition. However, we emphasize that our phase transition occurs not in equilibrium, but rather out of equilibrium in the driven NESS.

One may naively conclude from Fig. 2 that the phase transition requires extremely large QEPCs, which can be challenging to find experimentally. However, by solving the cubic equation, we find the following analytical expression for the critical driving frequency:

$$\omega_c = \sqrt{\omega_0^2 - \frac{2\sqrt{3}}{3}\gamma_{\text{ph}}\omega_0 + \frac{1}{2}\sqrt{\gamma_{\text{ph}}^4 - \frac{\pi t_0 \tilde{b}}{3g_q^2\omega_0} - 4\gamma_{\text{ph}}^2\omega_0^2 - \frac{96g_q^4\omega_0^4\mathcal{A}_0^2}{\pi^2 t_0^2 \tilde{b}}}}, \quad (5)$$

where  $\tilde{b} = g_q^2\omega_0\gamma_{\text{ph}}(3\gamma_{\text{ph}} - 4\sqrt{3}\omega_0)/\pi t_0$ . Importantly, this shows that a phase transition persists down to arbitrarily small  $g_q$ , as seen in the parametric plot of  $\gamma_{\text{ph}}$  vs.  $g_q$  in Fig. 3. Intriguingly, even with 1% damping of phonon energy ( $\gamma_{\text{ph}} \approx 0.048$  THz) to the phononic bath, governed by the Lindemann criterion [57], the system still features the phase transition for moderate QEPC  $g_q = \omega_0/2 = t_0$ . The region in which the transition can be observed increases with the phonon frequency.

The generalized force in Fig. 2(c) suggests that two stable equilibria exist at large  $g_q$  or small  $\omega$ , yet only one NESS is seen in our simulation for each value of the parameters. This is the attractor of the equations of motion starting from our initial ground state. To realize the other NESS, a different initial state must be prepared. Taking the cue from hysteresis near equilibrium first-order phase transitions, we suggest that this may be done via slowly ramping one of the parameters, such as the frequency (a “chirp” protocol). We consider a linearly chirped electric field  $\mathcal{E}(t) = \mathcal{A}_0 \cos(\omega(t)t)$  with  $\omega(t) = \omega_1 + (\omega_2 - \omega_1)(t - \tau_1)/(\tau_2 - \tau_1)$ , as shown in Fig. 4(a), inset. Such frequency ramps are important throughout

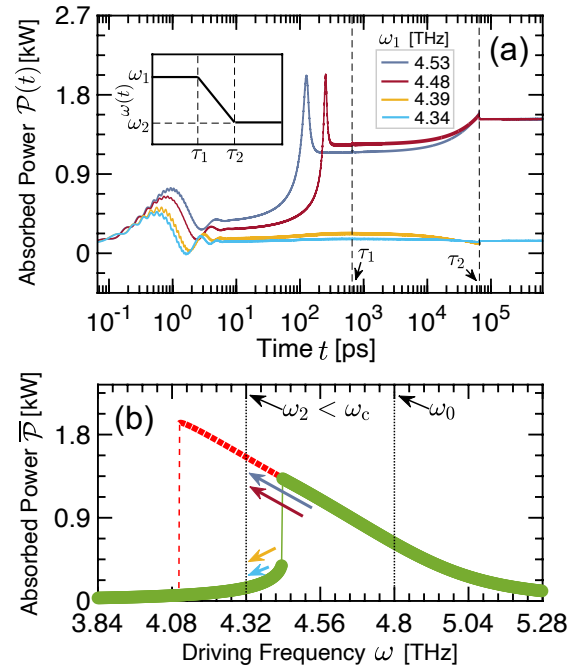


FIG. 4. **Chirp protocol for realizing the alternative steady state.** (a) Absorbed power in presence of a linearly chirped electric field  $\mathcal{E}(t) = \mathcal{A}_0 \cos(\omega(t)t)$  with  $\omega(t) = \omega_1 + [(\omega_2 - \omega_1)(t - \tau_1)/(\tau_2 - \tau_1)]$  (inset) for fixed  $\omega_2 = 4.32$  THz  $< \omega_c = 4.44$  THz. (b) Depending on whether  $\omega_1$  is less than or greater than  $\omega_c$ , the system ends up in a different branch of the steady state. Black arrows point to the positions of the frequencies  $\omega_0$  and  $\omega_2$  (black dotted vertical lines); color-coded arrows indicate the value of  $\omega_1$ , cf. legend in (a). Parameters are  $\omega_0 = 4.8$  THz,  $\mathcal{A}_0 = 0.036$  THz,  $\gamma_{\text{ph}} = 0.24$  THz, and  $\gamma_e = 0.0024$  THz.

ultrafast spectroscopy [58, 59], and can thus be implemented experimentally. Starting with frequency  $\omega_1$  at time  $\tau_1$  sufficiently large to reach the NESS, we slowly ramp to the final value  $\omega_2 < \omega_c$  at time  $\tau_2$ . If  $\omega_1 < \omega_c$  as well, no phase transition is crossed by this ramp and the system simply reaches the original NESS. However, if  $\omega_1 > \omega_c$ , the system instead stays in the upper NESS with large  $g_{\text{ph}}^2$ , as shown in Fig. 4(b). Similar hysteretic preparation of the alternative NESS can be accomplished via slowly ramping other experimental parameters, such as the drive amplitude  $\mathcal{A}_0$  in Fig. 1(b).

*Conclusion/Outlook.*—We have uncovered a novel nonequilibrium phase transition of a driven-dissipative fermion chain coupled to a phonon mode. By dynamically tuning the dissipation processes through the backaction of phononic excitations on the electronic dispersion, we find a robust phase transition from having a unique nonequilibrium steady state to having two stable steady states. Since the effect is favored by a quasi-equilibrium electron density (less than 2% deviation from a half-filled chain in equilibrium), it should be prevalent in any fermion chain. Our findings motivate future nonequilibrium spectroscopy experiments to seek photo-induced

phononic phase transitions in driven quantum materials such as driven superconductors, where the modified phononic steady state may enable a nonequilibrium pathway to controlling superconductivity [60, 61]. This phase transition will likely also be possible in the presence of an electromagnetic cavity, which has been used in recent work to control heating in driven materials [62–64].

*Acknowledgments.*—This work was performed with support from the National Science Foundation (NSF) through award numbers MPS-2228725 and DMR-1945529 and the Welch Foundation through award number AT-2036-20200401 (MK and MY). Part of this work was performed at the Aspen Center for Physics, which is supported by NSF grant No. PHY-1607611, and at the Kavli Institute for Theoretical Physics, which is supported by NSF grant No. NSF PHY-1748958. This project was funded by The University of Texas at Dallas Office of Research and Innovation through the SPIRE program. M.B. was supported by Marie Skłodowska Curie Grant No. 890711 (until 01.09.2022).

---

\* mohsen.yarmohammadi@utdallas.edu

† mgbukov@pks.mpg.de

‡ mkolodru@utdallas.edu

- [1] F. Novelli, G. De Filippis, V. Cataudella, M. Esposito, I. Vergara, F. Cilento, E. Sindici, A. Amaricci, C. Giannetti, D. Prabhakaran, S. Wall, A. Perucchi, S. Dal Conte, G. Cerullo, M. Capone, A. Mishchenko, M. Grüninger, N. Nagaosa, F. Parmigiani, and D. Fausti, Witnessing the formation and relaxation of dressed quasiparticles in a strongly correlated electron system, *Nature Communications* **5**, 5112 (2014).
- [2] S. Dal Conte, L. Vidmar, D. Golež, M. Mierzejewski, G. Soavi, S. Peli, F. Banfi, G. Ferrini, R. Comin, B. M. Ludbrook, L. Chauviere, N. D. Zhigadlo, H. Eisaki, M. Greven, S. Lupi, A. Damascelli, D. Brida, M. Capone, J. Bonča, G. Cerullo, and C. Giannetti, Snapshots of the retarded interaction of charge carriers with ultrafast fluctuations in cuprates, *Nature Physics* **11**, 421 (2015).
- [3] C. Giannetti, M. Capone, D. Fausti, M. Fabrizio, F. Parmigiani, and D. Mihailovic, Ultrafast optical spectroscopy of strongly correlated materials and high-temperature superconductors: a non-equilibrium approach, *Advances in Physics* **65**, 58 (2016).
- [4] D. N. Basov, R. D. Averitt, D. van der Marel, M. Dressel, and K. Haule, Electrodynamics of correlated electron materials, *Rev. Mod. Phys.* **83**, 471 (2011).
- [5] J. Orenstein, Ultrafast spectroscopy of quantum materials, *Physics Today* **65**, 44 (2012).
- [6] D. N. Basov, R. D. Averitt, and D. Hsieh, Towards properties on demand in quantum materials, *Nature Materials* **16**, 1077 (2017).
- [7] A. de la Torre, D. M. Kennes, M. Claassen, S. Gerber, J. W. McIver, and M. A. Sentef, Colloquium: Nonthermal pathways to ultrafast control in quantum materials, *Rev. Mod. Phys.* **93**, 041002 (2021).
- [8] I. Carusotto and C. Ciuti, Quantum fluids of light, *Rev. Mod. Phys.* **85**, 299 (2013).
- [9] E. I. R. Chiacchio and A. Nunnenkamp, Emergence of continuous rotational symmetries in ultracold atoms coupled to optical cavities, *Phys. Rev. A* **98**, 023617 (2018).
- [10] N. Lambert, S. Ahmed, M. Cirio, and F. Nori, Modelling the ultra-strongly coupled spin-boson model with unphysical modes, *Nature Communications* **10**, 3721 (2019).
- [11] M. Grätzel, Photoelectrochemical cells, *Nature* **414**, 338 (2001).
- [12] A. D. Wright, C. Verdi, R. L. Milot, G. E. Eperon, M. A. Pérez-Osorio, H. J. Snaith, F. Giustino, M. B. Johnston, and L. M. Herz, Electron–phonon coupling in hybrid lead halide perovskites, *Nature Communications* **7**, 11755 (2016).
- [13] M. Rini, R. Tobey, N. Dean, J. Itatani, Y. Tomioka, Y. Tokura, R. W. Schoenlein, and A. Cavalleri, Control of the electronic phase of a manganite by mode-selective vibrational excitation, *Nature* **449**, 72 (2007).
- [14] M. Mitrano, A. Cantaluppi, D. Nicoletti, S. Kaiser, A. Perucchi, S. Lupi, P. Di Pietro, D. Pontiroli, M. Riccò, S. R. Clark, D. Jaksch, and A. Cavalleri, Possible light-induced superconductivity in  $K_3C_{60}$  at high temperature, *Nature* **530**, 461 (2016).
- [15] M. Malinauskas, A. Žukauskas, S. Hasegawa, Y. Hayasaki, V. Mizeikis, R. Buividas, and S. Juodkazis, Ultrafast laser processing of materials: from science to industry, *Light: Science & Applications* **5**, e16133 (2016).
- [16] R. Mankowsky, M. Först, and A. Cavalleri, Non-equilibrium control of complex solids by nonlinear phononics, *Reports on Progress in Physics* **79**, 064503 (2016).
- [17] R. J. McQueeney, J. L. Sarrao, P. G. Pagliuso, P. W. Stephens, and R. Osborn, Mixed lattice and electronic states in high-temperature superconductors, *Phys. Rev. Lett.* **87**, 077001 (2001).
- [18] S. Tajima, Y. Fudamoto, T. Kakeshita, B. Gorshunov, V. Železný, K. M. Kojima, M. Dressel, and S. Uchida, In-plane optical conductivity of  $La_{2-x}Sr_xCuO_4$ : Reduced superconducting condensate and residual Drude-like response, *Phys. Rev. B* **71**, 094508 (2005).
- [19] L. Perfetti, P. A. Loukakos, M. Lisowski, U. Bovensiepen, H. Berger, S. Biermann, P. S. Cornaglia, A. Georges, and M. Wolf, Time evolution of the electronic structure of  $1T-TaS_2$  through the insulator-metal transition, *Phys. Rev. Lett.* **97**, 067402 (2006).
- [20] S. Hellmann, M. Beye, C. Sohrt, T. Rohwer, F. Sorgenfrei, H. Redlin, M. Källäne, M. Marczyński-Bühlow, F. Hennies, M. Bauer, A. Föhlisch, L. Kipp, W. Wurth, and K. Rossnagel, Ultrafast melting of a charge-density wave in the mott insulator  $1T-TaS_2$ , *Phys. Rev. Lett.* **105**, 187401 (2010).
- [21] S. Hellmann, T. Rohwer, M. Källäne, K. Hanff, C. Sohrt, A. Stange, A. Carr, M. M. Murnane, H. C. Kapteyn, L. Kipp, M. Bauer, and K. Rossnagel, Time-domain classification of charge-density-wave insulators, *Nature Communications* **3**, 1069 (2012).
- [22] T. Rohwer, S. Hellmann, M. Wiesenmayer, C. Sohrt, A. Stange, B. Slomski, A. Carr, Y. Liu, L. M. Avila, M. Källäne, S. Mathias, L. Kipp, K. Rossnagel, and M. Bauer, Collapse of long-range charge order tracked by time-resolved photoemission at high momenta, *Nature* **471**, 490 (2011).
- [23] C.-K. Chan, T. E. Lee, and S. Gopalakrishnan, Limit-

- cycle phase in driven-dissipative spin systems, *Phys. Rev. A* **91**, 051601 (2015).
- [24] R. M. Wilson, K. W. Mahmud, A. Hu, A. V. Gorshkov, M. Hafezi, and M. Foss-Feig, Collective phases of strongly interacting cavity photons, *Phys. Rev. A* **94**, 033801 (2016).
- [25] M. Yarmohammadi, C. Meyer, B. Fauseweh, B. Normand, and G. S. Uhrig, Dynamical properties of a driven dissipative dimerized  $S = \frac{1}{2}$  chain, *Phys. Rev. B* **103**, 045132 (2021).
- [26] M. Schiró, C. Joshi, M. Bordyuh, R. Fazio, J. Keeling, and H. E. Türeci, Exotic attractors of the nonequilibrium Rabi-Hubbard model, *Phys. Rev. Lett.* **116**, 143603 (2016).
- [27] J. Jin, D. Rossini, R. Fazio, M. Leib, and M. J. Hartmann, Photon solid phases in driven arrays of nonlinearly coupled cavities, *Phys. Rev. Lett.* **110**, 163605 (2013).
- [28] J. Jin, D. Rossini, M. Leib, M. J. Hartmann, and R. Fazio, Steady-state phase diagram of a driven qcd-cavity array with cross-Kerr nonlinearities, *Phys. Rev. A* **90**, 023827 (2014).
- [29] T. E. Lee, H. Häffner, and M. C. Cross, Antiferromagnetic phase transition in a nonequilibrium lattice of Rydberg atoms, *Phys. Rev. A* **84**, 031402 (2011).
- [30] M. Marcuzzi, E. Levi, S. Diehl, J. P. Garrahan, and I. Lesanovsky, Universal nonequilibrium properties of dissipative Rydberg gases, *Phys. Rev. Lett.* **113**, 210401 (2014).
- [31] C. D. Parmee and N. R. Cooper, Phases of driven two-level systems with nonlocal dissipation, *Phys. Rev. A* **97**, 053616 (2018).
- [32] R. Labouvie, B. Santra, S. Heun, and H. Ott, Bistability in a driven-dissipative superfluid, *Phys. Rev. Lett.* **116**, 235302 (2016).
- [33] M. Foss-Feig, P. Niroula, J. T. Young, M. Hafezi, A. V. Gorshkov, R. M. Wilson, and M. F. Maghrebi, Emergent equilibrium in many-body optical bistability, *Phys. Rev. A* **95**, 043826 (2017).
- [34] M. Biondi, G. Blatter, H. E. Türeci, and S. Schmidt, Nonequilibrium gas-liquid transition in the driven-dissipative photonic lattice, *Phys. Rev. A* **96**, 043809 (2017).
- [35] J. Bonča and S. A. Trugman, Dynamic properties of a polaron coupled to dispersive optical phonons, *Phys. Rev. B* **103**, 054304 (2021).
- [36] D. M. Kennes, E. Y. Wilner, D. R. Reichman, and A. J. Millis, Transient superconductivity from electronic squeezing of optically pumped phonons, *Nature Physics* **13**, 479 (2017).
- [37] J. Sous, B. Kloss, D. M. Kennes, D. R. Reichman, and A. J. Millis, Phonon-induced disorder in dynamics of optically pumped metals from nonlinear electron-phonon coupling, *Nature Communications* **12**, 5803 (2021).
- [38] See the Supplemental Materials at <http://xxx.yyy.zzz> for further details of the model Hamiltonian, corresponding equations of motion, resonance/off-resonance phononic and electronic responses, and energy flows.
- [39] T. K. Kim, A. A. Kordyuk, S. V. Borisenko, A. Koitzsch, M. Knupfer, H. Berger, and J. Fink, Doping dependence of the mass enhancement in  $(\text{Pb,Bi})_2\text{Sr}_2\text{CaCu}_2\text{O}_8$  at the antinodal point in the superconducting and normal states, *Phys. Rev. Lett.* **91**, 167002 (2003).
- [40] M. A. Sentef, Light-enhanced electron-phonon coupling from nonlinear electron-phonon coupling, *Phys. Rev. B* **95**, 205111 (2017).
- [41] M. Puviani and M. A. Sentef, Quantum nonlinear phononics route towards nonequilibrium materials engineering: Melting dynamics of a ferroelectric charge density wave, *Phys. Rev. B* **98**, 165138 (2018).
- [42] G. Lindblad, On the generators of quantum dynamical semigroups, *Comm. Math. Phys.* **48**, 119 (1976).
- [43] H. Breuer and F. Petruccione, *The Theory of Open Quantum Systems* (OUP Oxford, 2007).
- [44] M. Mitrano, G. Cotugno, S. R. Clark, R. Singla, S. Kaiser, J. Stähler, R. Beyer, M. Dressel, L. Baldassarre, D. Nicoletti, A. Perucchi, T. Hasegawa, H. Okamoto, D. Jaksch, and A. Cavalleri, Pressure-dependent relaxation in the photoexcited mott insulator  $\text{ET-F}_2\text{TCNQ}$ : Influence of hopping and correlations on quasiparticle recombination rates, *Phys. Rev. Lett.* **112**, 117801 (2014).
- [45] Z. Duan-Ming, F. Ran-Ran, L. Zhi-Hua, G. Li, L. Li, T. Xin-Yu, L. Dan, L. Gao-Bin, and H. De-Zhi, A new synthetic model of high-power pulsed laser ablation, *Communications in Theoretical Physics* **48**, 163 (2007).
- [46] E. Rowe, B. Yuan, M. Buzzi, G. Jotzu, Y. Zhu, M. Fechner, M. Först, B. Liu, D. Pontiroli, M. Riccò, and A. Cavalleri, Giant resonant enhancement for photo-induced superconductivity in  $\text{K}_3\text{C}_{60}$  (2023).
- [47] E. Wang, J. D. Adelinia, M. Chavez-Cervantes, T. Matsuyama, M. Fechner, M. Buzzi, G. Meier, and A. Cavalleri, Nonlinear transport in a photo-induced superconductor (2023).
- [48] P. E. Dolgirev, A. Zong, M. H. Michael, J. B. Curtis, D. Podolsky, A. Cavalleri, and E. Demler, Periodic dynamics in superconductors induced by an impulsive optical quench, *Communications Physics* **5**, 234 (2022).
- [49] A. von Hoegen, M. Fechner, M. Först, N. Taherian, E. Rowe, A. Ribak, J. Porras, B. Keimer, M. Michael, E. Demler, and A. Cavalleri, Amplification of superconducting fluctuations in driven  $\text{YBa}_2\text{Cu}_3\text{O}_{6+x}$ , *Phys. Rev. X* **12**, 031008 (2022).
- [50] M. Henstridge, M. Först, E. Rowe, M. Fechner, and A. Cavalleri, Nonlocal nonlinear phononics, *Nature Physics* **18**, 457 (2022).
- [51] M. Buzzi, D. Nicoletti, S. Fava, G. Jotzu, K. Miyagawa, K. Kanoda, A. Henderson, T. Siegrist, J. A. Schlueter, M.-S. Nam, A. Ardavan, and A. Cavalleri, Phase diagram for light-induced superconductivity in  $\kappa\text{-(ET)}_2\text{-X}$ , *Phys. Rev. Lett.* **127**, 197002 (2021).
- [52] M. Buzzi, G. Jotzu, A. Cavalleri, J. I. Cirac, E. A. Demler, B. I. Halperin, M. D. Lukin, T. Shi, Y. Wang, and D. Podolsky, Higgs-mediated optical amplification in a nonequilibrium superconductor, *Phys. Rev. X* **11**, 011055 (2021).
- [53] M. Buzzi, D. Nicoletti, M. Fechner, N. Tancogne-Dejean, M. A. Sentef, A. Georges, T. Biesner, E. Uykur, M. Dressel, A. Henderson, T. Siegrist, J. A. Schlueter, K. Miyagawa, K. Kanoda, M.-S. Nam, A. Ardavan, J. Coulthard, J. Tindall, F. Schlwin, D. Jaksch, and A. Cavalleri, Photomolecular high-temperature superconductivity, *Phys. Rev. X* **10**, 031028 (2020).
- [54] Note that the phonon relaxation is not modified because it remains gapped throughout the simulations at zero temperature.
- [55] R. Dann, A. Levy, and R. Kosloff, Time-dependent Markovian quantum master equation, *Phys. Rev. A* **98**, 052129 (2018).

- [56] S. L. Johnson, P. Beaud, E. Vorobeva, C. J. Milne, E. D. Murray, S. Fahy, and G. Ingold, Directly observing squeezed phonon states with femtosecond x-ray diffraction, *Phys. Rev. Lett.* **102**, 175503 (2009).
- [57] F. A. Lindemann, The calculation of molecular vibration frequencies, *Phys. Z.* **11**, 609 (1910).
- [58] D. Seipt, V. Y. Kharin, and S. G. Rykovanov, Optimizing laser pulses for narrow-band inverse Compton sources in the high-intensity regime, *Phys. Rev. Lett.* **122**, 204802 (2019).
- [59] V. Y. Kharin, D. Seipt, and S. G. Rykovanov, Higher-dimensional caustics in nonlinear Compton scattering, *Phys. Rev. Lett.* **120**, 044802 (2018).
- [60] C. J. Eckhardt, S. Chattopadhyay, D. M. Kennes, E. A. Demler, M. A. Sentef, and M. H. Michael, Theory of resonantly enhanced photo-induced superconductivity (2023).
- [61] S. Chattopadhyay, C. J. Eckhardt, D. M. Kennes, M. A. Sentef, D. Shin, A. Rubio, A. Cavalleri, E. A. Demler, and M. H. Michael, Mechanisms for long-lived, photo-induced superconductivity (2023).
- [62] F. Schlawin, D. M. Kennes, and M. A. Sentef, Cavity quantum materials, *Applied Physics Reviews* **9**, 011312 (2022).
- [63] M. A. Sentef, M. Ruggenthaler, and A. Rubio, Cavity quantum-electrodynamical polaritonically enhanced electron-phonon coupling and its influence on superconductivity, *Science Advances* **4**, eaau6969 (2018).
- [64] B. L. Dé, C. J. Eckhardt, D. M. Kennes, and M. A. Sentef, Cavity engineering of Hubbard  $U$  via phonon polaritons, *Journal of Physics: Materials* **5**, 024006 (2022).